Analytica Chimica Acta 1230 (2022) 340357

Contents lists available at ScienceDirect

Analytica Chimica Acta

journal homepage: www.elsevier.com/locate/aca

Aptamer-based colorimetric detection of methicillin-resistant *Staphylococcus aureus* by using a CRISPR/Cas12a system and recombinase polymerase amplification

Luyu Wei [a], Zhilong Wang [a], Jia Wang [a], Xiaohong Wang [a], Yiping Chen [a,b,c,d,*]

[a] Key Laboratory of Environment Correlative Dietology, Huazhong Agricultural University, Ministry of Education, Wuhan, 430070, Hubei, China
[b] Guangdong Laboratory for Lingnan Modern Agriculture, Guangzhou, 510642, Guangdong, China
[c] Shenzhen Institute of Nutrition and Health, Huazhong Agricultural University, Wuhan, 430070, Hubei, China
[d] Shenzhen Branch, Guangdong Laboratory for Lingnan Modern Agriculture, Genome Analysis Laboratory of the Ministry of Agriculture, Agricultural Genomics Institute at Shenzhen, Chinese Academy of Agricultural Sciences, Shenzhen, Guangdong, 518120, China

HIGHLIGHTS

- A simple aptamer-based colorimetry was developed for sensitive detection of MRSA.
- The aptamer is used as the substrate of *trans*-cleavage and modulator of colorimetry.
- With the triple amplification, MRSA as low as 8 CFU mL^{-1} was detected.
- The method has potential as a robust drug-resistant bacteria detection platform.

GRAPHICAL ABSTRACT

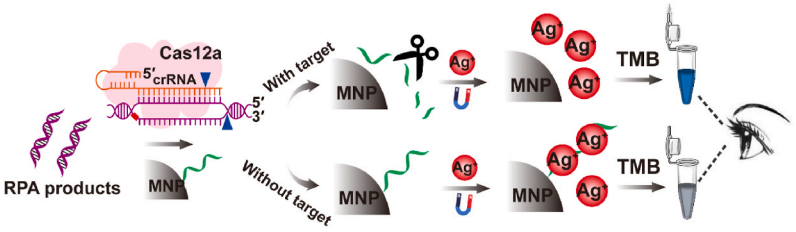

ARTICLE INFO

Keywords:
CRISPR/Cas12a
Methicillin-resistant *Staphylococcus aureus*
Colorimetric analysis
Aptamer
Ag^+-TMB system

ABSTRACT

Detection of methicillin-resistant *Staphylococcus aureus* (MRSA) with superior accuracy, timeliness, and simplicity is highly valuable in clinical diagnosis and food safety. In this study, an aptamer-based colorimetric biosensor was developed to detect MRSA by using a CRISPR/Cas12a system and recombinase polymerase amplification (RPA). The aptamer of silver ion (Ag^+) pre-coupled to magnetic nanoparticles was employed not only as the substrate of *trans*-cleavage in the CRISPR/Cas12a system, but also as the modulator of Ag^+–3,3′,5,5′-tetramethylbenzidine (TMB) chromogenic reaction, innovatively integrating the powerful CRISPR/Cas12a system with convenient colorimetry. The utilized aptamer containing consecutive and interrupted cytosine: cytosine mismatched base pairs also served as a signal amplifier because of the one-to-multiple binding of the aptamer to Ag^+. Using triple amplification of RPA, multiple-turnover nuclease activity of Cas12a, and cytosine–Ag^+–cytosine coordination chemistry, MRSA was detected as low as 8 CFU mL^{-1}. Moreover, its satisfactory accuracy in the analysis of real samples, together with visualization and simplicity, revealed the great potential of the proposed biosensor as a robust antibiotic-resistant bacteria detection platform.

* Corresponding author. Key Laboratory of Environment Correlative Dietology, Huazhong Agricultural University, Ministry of Education, Wuhan, 430070, Hubei, China.
E-mail addresses: wly2025@163.com (L. Wei), wzl186@webmail.hzau.edu.cn (Z. Wang), wangjia@mail.hzau.edu.cn (J. Wang), wxh@mail.hzau.edu.cn (X. Wang), chenyiping@mail.hzau.edu.cn (Y. Chen).

https://doi.org/10.1016/j.aca.2022.340357
Received 10 April 2022; Received in revised form 31 August 2022; Accepted 2 September 2022
Available online 13 September 2022

1. Introduction

Methicillin-resistant *Staphylococcus aureus* (MRSA) is one of the antibiotic-resistant bacteria that cause infections such as pneumonia [1,2], bacteremia [3], and endocarditis [4]. Rapid and accurate diagnosis of MRSA is the prerequisite for proper infection treatment. Due to its simplicity, antimicrobial susceptibility testing is conventionally used as the gold standard for MRSA detection [5,6]; however, time costs and false-negative results impede its application. The use of an expensive antibody hinders the application of immunological methods despite its satisfactory specificity [7]. Emerging approaches based on nucleic acids seem more advantageous over other methods because of the direct identification of the associated antibiotic resistance genes. General polymerase chain reaction (PCR) [8] and PCR-based [9,10] and emerging isothermal amplification methods, such as loop-mediated isothermal amplification [11] and nucleic acid sequence-based amplification [12], possess satisfactory sensitivity. However, the PCR-based method involves sophisticated equipment and precise temperature cycling, whereas isothermal amplification methods are not available to detect a single nucleotide. Therefore, the development of a sensitive, specific, rapid, and convenient nucleic acid-based strategy for MRSA detection is crucial.

Clustered regularly interspaced short palindromic repeats (CRISPR) and CRISPR-associated proteins (Cas) are adaptive immune systems that were first found in bacteria and archaea [13]. Although the development history of CRISPR-based diagnosis covers a period shorter than 5 years only, it largely advanced molecular diagnostics of diverse targets. Among its various types, the class 2 type V-A CRISPR/Cas12a (Cpf1) [14] is widely used in nucleic acid biosensing and clinical diagnosis. Compared to the conventional CRISPR/Cas9 system that only cleaves target DNA, the target DNA-activated RNA-guided CRISPR/Cas12a system can indiscriminately cleave any nontarget single-stranded DNA (ssDNA, termed *trans*-cleave) [15]. Significantly, the *trans*-cleavage of Cas12a is multiple-turnover, making it capable of being harnessed for the amplified detection of nucleic acid targets. In addition, Cas12a has a higher specificity than the currently widely used Cas9. Site-specific recognition and indiscriminate single-strand DNase activity of CRISPR/Cas12a impart ultrahigh specificity (single-nucleotide resolution) and sensitivity (single-molecule levels) to nucleic acid detection. Various CRISPR/Cas12a-based nucleic acid detection thus far include fluorescence assay [16,17], lateral flow assay [18,19], electrochemical methods [20], surface-enhanced Raman scattering (SERS) [21], digital microfluidics [22,23], and colorimetry [24–26], and so on [27,28]. Due to their device independence, affordability, and visualization, CRISPR/Cas12a-based colorimetric methods exhibit the most potential for in-field application. These methods commonly use gold nanoparticles (AuNPs) as a signal probe and ssDNA as a smart material to regulate their dispersion and aggregation for studying color change. Despite great success, this ssDNA-regulated state alteration of AuNPs is usually realized by DNA hybridization, which is one-to-one signal transduction, and its sensitivity is insufficient to detect MRSA with high requirements for sensitivity. Therefore, an effective alternative that

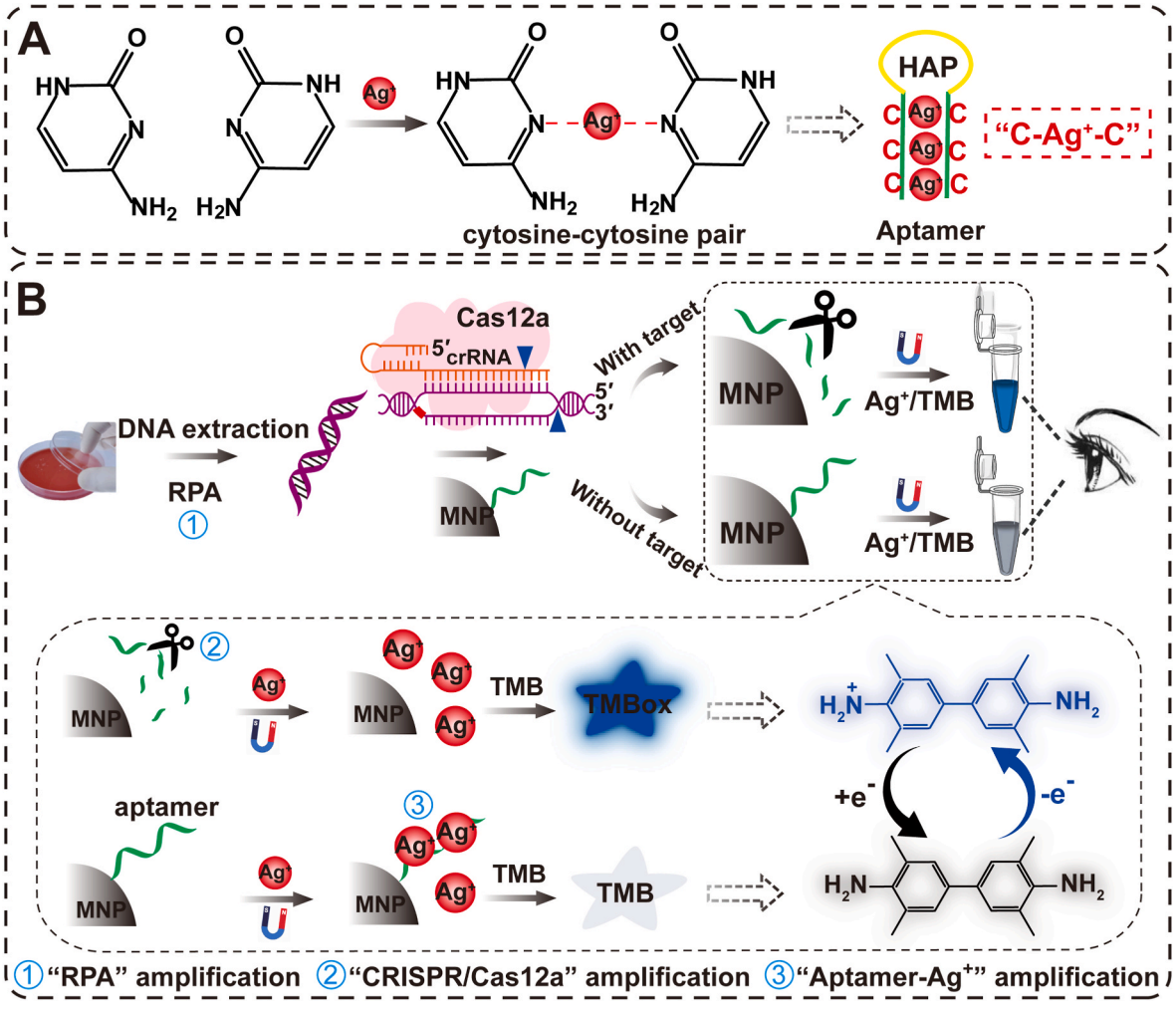

Scheme 1. Schematic of aptamer-based colorimetric biosensor using a CRISPR/Cas12a system and RPA. (A) Schematic of binding between aptamer and Ag^{+}. (B) Schematic of MRSA detection by aptamer-based colorimetric biosensor using the CRISPR/Cas12a system and RPA.

exhibits simplicity and desired sensitivity is needed.

In the current study, an aptamer-based colorimetric biosensor was developed for the rapid, ultrasensitive, and visual detection of MRSA using the CRISPR/Cas12a system and recombinase polymerase amplification (RPA). In this sensing strategy, an aptamer was employed to chelate silver ions (Ag^+) by the interaction between Ag^+ and the N3 of cytosine (C), which bridge two cytosine residues to form a strong and stable "C–Ag^+-C" hairpin structure [29–31] (Scheme 1A). Meanwhile, this aptamer can be used as a substrate of CRISPR/Cas12a *trans*-cleavage due to its characteristic as an ssDNA. Specifically, DNA extracted from clinically isolated colonies was first amplified by RPA and further recognized by the CRISPR/Cas12a system. In the presence of MRSA, it activated Cas12a to *cis*-cleave the target DNA and remains bound to one of the resulting DNA fragments. This *cis*-cleavage event causes a Cas12a conformational shift that enables a second, nonspecific *trans*-cutting of the aptamer, resulting in the degradation of the aptamer pre-coupled to magnetic nanoparticles (Apt–MNPs). By magnetic separation, the sediment would only comprise MNPs. Furthermore, one of the organic dyes that can be oxidized by Ag^+, 3,3′,5,5′-tetramethylbenzidine (TMB), was used as a visualization probe. Thus, Ag^+ could not bind to the aptamer and instead reacted with TMB for coloring. In this situation, the solution containing oxidized TMB (TMBox) exhibited a blue coloration and a characteristic UV–vis absorption peak at 652 nm. In the absence of MRSA, accessory-cutting would not occur and the aptamer would still be intact and pulled down via a magnetic rack. By this process, Ag^+ can bind to the magnetically enriched aptamer by interacting with cytosine to form a "C–Ag^+-C" hairpin structure, the solution then becomes colorless without TMBox (Scheme 1B). In this strategy, the aptamer functions for the first time as both an amplifier and a connector for signal amplification and signal readout. In comparison to AuNP-based CRISPR diagnostics, the used aptamer contains numerous cytosine residues that can bind to multiple Ag^+; in addition, the preparation of TMB is repeatable and simple, thus has the priority in sensitivity and simplicity in MRSA detection. Benefiting from efficient integration and triple signal amplification of "RPA", "CRISPR/Cas12a" and "aptamer-Ag^+", this aptamer-based colorimetric biosensor can be a suitable candidate for the specific analysis of antibiotic-resistant bacteria.

2. Methods

2.1. Materials and instrumentation

Engen® Lba Cas12a (Cpf1, 100 μM) was purchased from New England Biolabs. SYBR® Premix Ex TaqTM II reaction mixture was purchased from TaKaRa. The 2 × T5 Super PCR Mix was purchased from Tsingke Biological Technology Company. The basic nucleic acid amplification reagent was purchased from Hangzhou ZC Bio-Sci&Tech Co., Ltd. (Hangzhou, China). The rapid bacterial genomic DNA isolation kit, RNase A inhibitor, and all nucleic acid sequences (Table S1) were supplied by Sangon Biotech (Shanghai, China). 3,3′,5,5′-tetramethylbenzidine (TMB, ≥99%, HPLC) and silver nitrate ($AgNO_3$) were obtained from Shanghai Macklin Biochemical Technology Co., Ltd. (Shanghai, China). Carboxyl-modified magnetic nanoparticles (COOH-MNPs) (1000 nm, 10 mg/mL) were purchased from Invitrogen (USA). 1-ethyl-3-(3-dimethylaminopropyl)-carbodiimide hydrochloride (EDC), 2-[N-morpholino] ethane sulfonic acid (MES), 2-Amino-2-(hydroxymethyl) propane-1,3-diol (Tris), Tween-20, ethylene diamine tetraacetic acid (EDTA) and other chemicals were purchased from Sigma-Aldrich (USA). All chemicals and reagents used were of analytical grade. *Salmonella enteritidis* (*S. enteritidis*, ATCC 13076), *Escherichia coli* (*E. coli*, ATCC 25922), *Listeria monocytogenes* (*L. monocytogenes*, ATCC 43257) and methicillin-susceptible *Staphylococcus aureus* (MSSA, ATCC 29213) were obtained from the American Type Culture Collection (ATCC). Trypticase soy broth (TSB) was purchased from Qingdao Hope Bio-Technology Co., Ltd. (Qingdao, China). Ultrapure water (resistivity ≥18.3 MΩ cm) was used in the experiments. Twelve suspected MRSA colonies were isolated from clinical samples at a hospital in Wuhan (China).

The SuperMag magnetic separator was purchased from Ocean NanoTech (USA). Fluorescence data was collected by multi-model microplate reader (BioTek Synergy HTX) using 485 nm excitation and 520 nm emission. Thermal cycler (Bio-Rad, T100), gel imager (Bio-Rad, Gel Doc XR+), microvolume spectrophotometer (Implen, N60 Touch), microplates (384 wells, low volume, non-binding surface, black with clear flat bottom (Corning, Cat. nos. 3544) were used. The absorbance was measured using a UV–vis spectrophotometer (Thermo Scientific). Electrophoresis was performed on Beijing JUNYI-Dongfang electrophoresis equipment Co., Ltd. (JY300HC). The qPCR assay was performed on the Real-Time PCR System (Jena, Qtower 2.2).

2.2. Nucleic acid preparation

The target DNA for a proof of concept was ordered as two complementary ssDNA molecules and hybridized as the following procedure: the hybridization mixture was first prepared by combining 0.5 μL of 5 M NaCl, 5 μL of 10 × TE buffer and 22.5 μL of 100 μM ssDNA 1 and ssDNA 2. Then the two ssDNA sequences were annealed by performing a 5 min denaturation and the reaction was slowly cooled to 4 °C in a PCR thermal cycle. For slow cooling of the samples, the ramp rate was adjusted to 0.04 °C/s. The hybridized DNA can be used immediately or divided into aliquots and stored at −20 °C for up to several months.

Plasmid DNA was constructed by cloning partial *mecA* gene into the pUC57 vector, and the sequence is shown in Table S1. In real samples analysis, bacterial cells from suspected MRSA colonies were first grown in TSB medium at 37 °C until the optical density of the culture at 600 nm reached 0.7. Then 1 mL of bacterial suspension was pipetted to extract total genomic DNA using the rapid bacterial genomic DNA isolation kit, the products were divided into aliquots and stored at −20 °C for future use.

2.3. Preparation of aptamer-functionalized MNPs

The COOH-MNPs were first resuspended by rolling the vial for 30 min. Then 1 mL of them was transferred to a new tube and placed on a magnet for 2 min to remove the supernatant. Subsequently, COOH-MNPs were washed twice with 1 mL of MES buffer (100 mM, pH 4.8) and resuspend in 100 μL of the same buffer. In a separate tube, 5′ amine modified aptamer (5 nmol) and 40 μL of 1.25 M EDC in MES buffer were mixed to a total volume of 100 μL. This aptamer/EDC solution was added to the COOH-MNP and mixed by vortex for 10 s. The suspension was incubated on a roller mixer at room temperature for 3 h. Finally, the complex was washed 3 times again with 1 mL of TT buffer (1 M Tris-HCl, pH 8.0, containing 10% Tween-20) (each round incubated 30 min) and resuspended in TE buffer (1 M Tris-HCl, pH 8.0, containing 100 mM EDTA). The prepared aptamer-functionalized MNPs (Apt–MNPs) were stored at 4 °C for further use.

2.4. Recombinase polymerase amplification

Primers for recombinase polymerase amplification (RPA) were designed using NCBI Primer-BLAST. All RPA primers are listed in Table S1. The RPA reactions run as instructed with a Basic nucleic acid amplification reagent. 50 μL reactions containing 41.5 μL of A buffer, 2 μL of plasmid DNA with concentrations from 10 nM to 1 aM or extracted DNA, 2 μL of 10 μM forward and reverse primer, and 2.5 μL of B buffer were sequentially added to the reaction dry power-presenting tube, followed by incubation at 39 °C for 30 min. After amplification, 50 μL of DNA extraction reagents (saturated phenol: chloroform: isopentyl alcohol = 25: 24: 1) were added to the reaction solution, gently vortexed and thoroughly mixed. Following centrifugation at 10,000 r/min for 2 min, 5 μL of supernatant was used for agarose gel electrophoresis to determine the optimal primer set. For subsequent fluorescence and

colorimetric signal readout, 5 μL of the RPA reaction solution was transferred to CRISPR/Cas12a system as template.

2.5. CRISPR/Cas12a-based fluorescence detection

A calibration curve was prepared with the series of diluted plasmid DNA present at decreasing concentrations between 100 nM and 0.5 fM. First, Cas12a (200 nM) and gRNA (250 nM) were mixed in 1 × NE buffer r2.1 at 37 °C for 15 min, followed by the preparation of another signal mixture which contains 1 × NE buffer r2.1, 1 μM quenched, fluorescently labeled reporter ssDNA and amplicons. Then 5 μL of the Cas12a-gRNA complex and 15 μL of signal mixture were transferred to the 384-well microplate to obtain final concentrations of 50 nM Cas12a, 62.5 nM gRNA and 750 nM FQ reporter in 1 × NE buffer r2.1. Twenty microliters of mixture were incubated in a 384-well microplate in the microplate reader. Fluorescence readings were recorded every 5 min (excitation: 485 nm; emission: 520 nm) for 120 min at 37 °C.

2.6. Aptamer-based colorimetric detection of MRSA

The Cas12a-gRNA complex was assembled by incubating Cas12a (200 nM) with gRNA (250 nM) in 1 × NE buffer r2.1 at 37 °C for 15 min. Subsequently, the Cas12a-gRNA complex was mixed with 5 μL of different concentrations of double-stranded DNA trigger (without RPA) or 5 μL of RPA reaction solution (with RPA) and 25 μL of Apt–MNPs in a 1.5 mL centrifuge tube, then they were reacted at 37 °C for 15 min. After magnetic separation and washing twice with ultrapure water, 25 μL of 5 mM $AgNO_3$ were added and reacted at 37 °C for 10 min. Then 35 μL of 5 mM TMB was added to the mixture and reacted at room temperature for 25 min again with light-avoidance. Finally, absorbance at 652 nm was measured while coloration can be easily observed by the naked-eye. The limit of detection (LOD) was calculated based on the calibration curve with $3S/M$, where S is the value of the standard deviation of blank samples and M is the slope of the standard curve at a low concentration range.

2.7. PCR and qPCR assays

PCR was performed on Thermal cycler (Bio-Rad, T100). 1 μL of extracted DNA from 12 suspected samples were employed as the template, following the program: initial denaturation at 98 °C for 2 min, then 98 °C for 10 s, 59 °C 13 s, and 72 °C 10 s for 30 cycles, followed by final extension of 72 °C for 2 min. The PCR products were run on 1% agarose gel electrophoresis for 45 min with a voltage of 100 V to preliminarily judge whether the sample is positive or negative.

The sensitivity of the qPCR method with SYBR Green was tested using a dilution series of plasmid DNA (from 1 nM to 1 aM) as the template. The assay was performed on the Real-Time PCR System (Jena, Qtower 2.2) with the same program as PCR. For real sample analysis, genomic DNA extracted from suspected samples was qualified according to the amplification curve.

3. Results and discussion

Ag^+ can oxidize colorless TMB to colored TMBox. TMBox is a one-electron transfer product of TMB, showing blue coloration while exhibiting characteristic UV–vis absorption at 652 nm [32]. Ag^+ also selectively coordinates cytosine residues via N–Ag bonds to form the "C–Ag^+-C" pair [30]. Therefore, when there exists an aptamer of Ag^+ containing numerous cytosine residues, the original free Ag^+ in the solution is reduced because of aptamer binding, resulting in correspondingly decreased interaction with TMB. With this principle, the chromogenic reaction of Ag^+-TMB can be modulated using the aptamer.

In this study, three aptamers were used to investigate the effect of aptamer sequence on UV–vis absorption of the colorimetric system: two of the aptamers have been reported in the literature (Aptamer 1 and Aptamer 2) [30,31], while the other one was designed by ourselves (Aptamer 3) (Table S1). The optimal aptamer sequence was Aptamer 2: CCTCCCTCCCTCCCTTTTTCCCACCCACCCACC (Fig. S1), which performed better than Aptamer 1 and was more cost-effective than Aptamer 3. The interaction between Ag^+ and multiple aligned C: C mismatched base pairs, Ag^+ specifically bound to each C: C mismatched base pair at a 1: 1 M ratio with 10^6 M/L binding constant [33,34], demonstrating the high affinity and specificity of the employed aptamer for Ag^+. The oxidative ability of aptamer-bound Ag^+ on TMB was then explored. MNPs were introduced as a vehicle for separating aptamer-bound and -unbound Ag^+. Aptamer-bound Ag^+ was removed by magnetic separation, leaving only free Ag^+ to react with TMB. The successful preparation of Apt–MNPs was characterized by a zeta potential analysis (Fig. S2), in which the decreased potential was attributed to the conjugation of a negatively charged aptamer. Notably, no difference in characteristic UV–vis absorption of colorimetric solution was observed between the "with magnetic separation" and "without magnetic separation" (Fig. 1A), suggesting that the same amount of Ag^+ involved in chromogenic reaction in the two cases, and aptamer-bound Ag^+ could no longer react with TMB. Unlike free Ag^+, the aptamer-bound Ag^+ cannot oxidize TMB, and the separation of the aptamer-bound Ag^+ and free Ag^+ was unnecessary. Moreover, the signal readout of this aptamer-modulated colorimetry is homogeneous, simplifying the detection procedure.

The effect of this aptamer-modulated colorimetry was then evaluated. In the proposed strategy, the aptamer acts as a connector between signal recognition and signal readout. On the one hand, it serves as substrates for connecting the CRISPR/Cas12a signal recognition system. On the other hand, it can affect the colorimetric readout of Ag^+-TMB system by interacting with Ag^+. Thus, an excellent signal response upon slight variations in the aptamer is vital for ensuring the sensitivity of the method. In this study, the aptamer containing 11 consecutive and interrupted double C: C mismatched base pairs was employed; theoretically, numerous Ag^+ would be constrained in the formed secondary hairpin structure of the aptamer via "C–Ag^+-C" coordination chemistry. With this one-to-multiple binding feature of the aptamer to Ag^+, "aptamer–Ag^+" can act as an efficient signal amplifier. The optical response of different volumes of Apt–MNPs (0, 5, 10, 15, 20, 25, 30, and 45 μL) were thus examined. The results showed that the coloration of the solution gradually changed from dark blue to white as the volume of Apt–MNPs increased (Fig. 1B), and the ultraviolet absorbance at 652 nm was inversely proportional to the volume of the Apt–MNPs present (Fig. 1C and D). This occurrence was mainly attributed to the presence of more Ag^+ interacting with cytosine residues; meanwhile, less was used for colorimetry. Ag^+ and TMB dosages were also optimized, and the best analytical performance was observed in 5 mM $AgNO_3$ and 5 mM TMB (Fig. S3).

3.1. Feasibility of aptamer-based colorimetry using the CRISPR/Cas12a system

In MRSA, the primary mechanism for antibiotic resistance is the acquisition of a mobile cassette of genes known as the staphylococcal cassette chromosome *mec* (SCC*mec*). Within this cassette is the *mecA* gene that endows β-lactams, including methicillin, with resistance [35,36]. Thus, this extensively reported antibiotic-resistant gene of MRSA, *mecA*, was chosen as the target nucleic acid. In this study, a 20 bp target sequence in *mecA* adjacent to a TTTG protospacer adjacent motif (PAM) site was recognized by the complementary gRNA of the CRISPR/Cas12a system (Fig. 2A). Guided by the PAM sequence, the gRNA of CRISPR/Cas12a specifically recognized the target sequence, which would induce the alteration of Cas 12a. The effectiveness of the designed gRNA was first verified using the fluorescence method. Strong fluorescence was observed when a target was present (Fig. 2B), indicating that the programmed gRNA could be assembled with Cas12a and specifically recognized the target sequence.

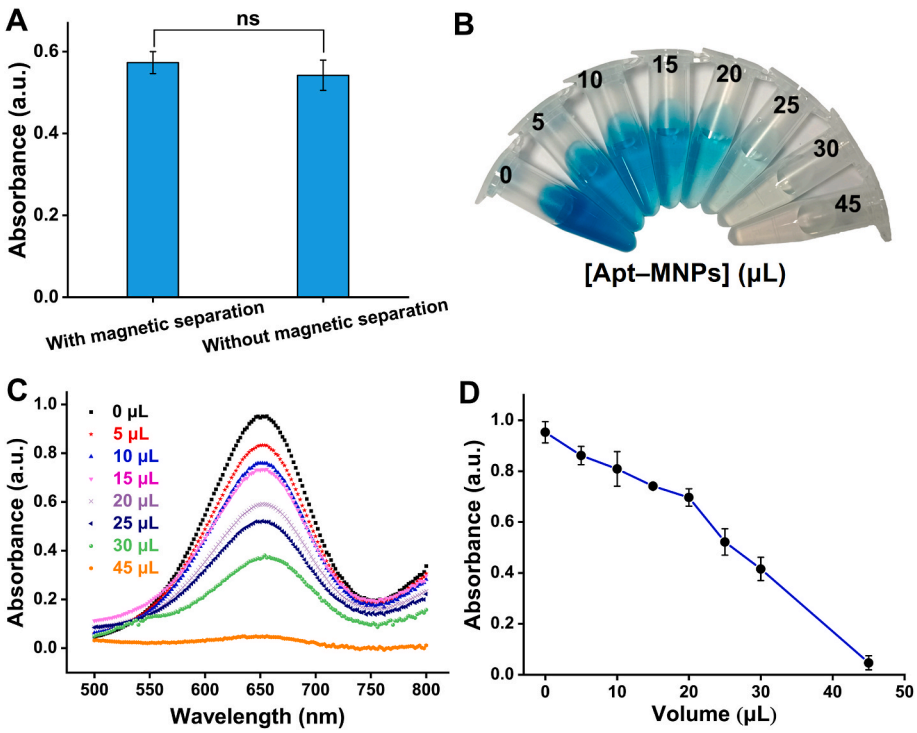

Fig. 1. Feasibility of aptamer-modulated colorimetry. (A) UV–vis absorption at 652 nm of the aptamer-modulated colorimetric system with and without magnetic separation, "ns" represents no significance. Photograph (B), UV–vis analysis (C), and UV–vis absorption at 652 nm (D) of a colorimetric system with different volumes of Apt–MNPs. $\Delta A = A\text{-}A_0$, A represents the absorbance at 652 nm in the presence of target, A_0 represents the absorbance at 652 nm in the absence of target. Error bars represent the standard deviation of three replicates (n = 3).

For a proof-of-concept, aptamer-based colorimetric detection of MRSA was performed using the CRISPR/Cas12a system. To achieve the desired detection results, several critical parameters were explored, including *trans*-cleavage time and volume of Apt–MNPs. The *trans*-cleavage time is particularly important for analytical performance. This time should be limited between the uncut and the complete cut, and the optimal time point should be determined. With longer time, the cleavage was excessive, hence the thorough degradation of the aptamer. Thus, no C base was conjugated in MNPs, and Ag^+ was entirely reacted with TMB. With shorter time, the difference in cleavage as a function of the target was not exhibited, causing a change in Ag^+ irrespective of the target. As such, unsuitable *trans*-cleavage time cannot allow the aptamer to change with the target and thus cannot modulate the subsequent colorimetry ideally. The *trans*-cleavage of the aptamer over different lengths of cleavage time was evaluated by using UV–vis analysis and 12% denatured polyacrylamide gel electrophoresis. Based on the experimental results, the desired result was obtained in 15 min of *trans*-cleavage time (Fig. 2C and D). In addition, 25 μL of Apt–MNPs provided not only the optimal optical response but also the least reagent usage, which was used in the subsequent experiments (Fig. S4).

Under optimal conditions, different concentrations of the double-stranded DNA (dsDNA) trigger (0, 0.1, 0.5, 5, 20, 80, 200, and 400 nM) were used to activate the collateral cleavage activity of Cas12a. As shown in Fig. 2E, the aptamer in the trigger-presenting lane is digested into random short fragments, unlike the opposite counterpart. This aptamer digestion was gradually strengthened with increased dsDNA trigger, confirming that aptamer was cleaved. The results of aptamer-based colorimetry revealed color darkening and an increase in absorbance at 652 nm as the dsDNA trigger increased from 0.5 nM (Fig. 2F). The occurrence was mainly attributed to the weak binding between the cleaved aptamer and Ag^+, resulting in more Ag^+ reacting with TMB for coloring. These results revealed the feasibility of the constructed aptamer-based colorimetric biosensor using the CRISPR/Cas12a system.

3.2. Sensitivity and specificity of aptamer-based colorimetric biosensor

To further improve sensitivity, the equipment-free, time-saving, and simple RPA was deployed for target amplification. Standard PCR was first used to select a positive sample as a positive control (named P) (Fig. S5). Subsequently, three pairs of primers targeting *mecA* gene were designed, and their amplification efficiencies were evaluated by agarose gel electrophoresis. As shown in Fig. 3A, both Primer 1 and Primer 3 lead to amplified DNA bands, Primer 1 has the strongest band, hence its selection for RPA amplification. Amplification-enhanced colorimetry was then performed to detect the *mecA* gene with three replicates, each with 10^7–10^{-3} fM plasmid DNA. The results showed that with RPA, 10 aM and 100 aM plasmid DNA can be reliably detected by UV–vis analysis and naked-eye observation, respectively. By contrast, this colorimetric biosensor without RPA could only detect 0.1 nM of plasmid DNA by UV–vis analysis (Fig. 3B). The sensitivity of this RPA-assisted colorimetric biosensor (10 aM) increased by seven orders of magnitude than that without PRA (0.1 nM), demonstrating the effectiveness of RPA signal amplification. Similarly, 10 CFU mL^{-1} MRSA can be quantified with a linear range of 10 CFU mL^{-1} to 10^5 CFU mL^{-1}. The correlation equation is $Y = 0.064X + 0.094$ {X = log [MRSA] (CFU mL^{-1}), R^2 = 0.98} with a LOD of 8 CFU mL^{-1} ($S = 0.184$, $M = 0.072$) (Fig. 3C). The sensitivity of RPA-amplified CRISPR/Cas12a-based fluorimetry and qPCR method for *mecA* gene detection was also assessed for comparison (Fig. S6). The proposed method mainly resulting from triple amplification exhibited sensitivity that was comparable or superior to that of CRISPR/Cas12a-based fluorimetry and qPCR method.

Compared to previously reported CRISPR-based colorimetry (Table S2), the sensitivity of this aptamer-based colorimetric biosensor is superior to another CRISPR-mediated lateral flow assay and inferior to the plasmonic AuNPs-based CRISPR method. The higher sensitivity of the plasmonic AuNPs-based CRISPR method is attributed to the higher molar extinction coefficient of AuNPs than the TMB that was used in our study. However, the AuNPs-based CRISPR method exhibits a "signal-off" detection mode, in which the color changes from red to blue. Differently, our method presented an opposite "signal-on" detection format—that is, a colorless-to-blue color change which is more easily perceived. Compared with classical CRISPR-based instrumental method such as CRISPR-based SERS and electrochemical method (Table S2), the sensitivity of our method increased by two orders of magnitude and one order

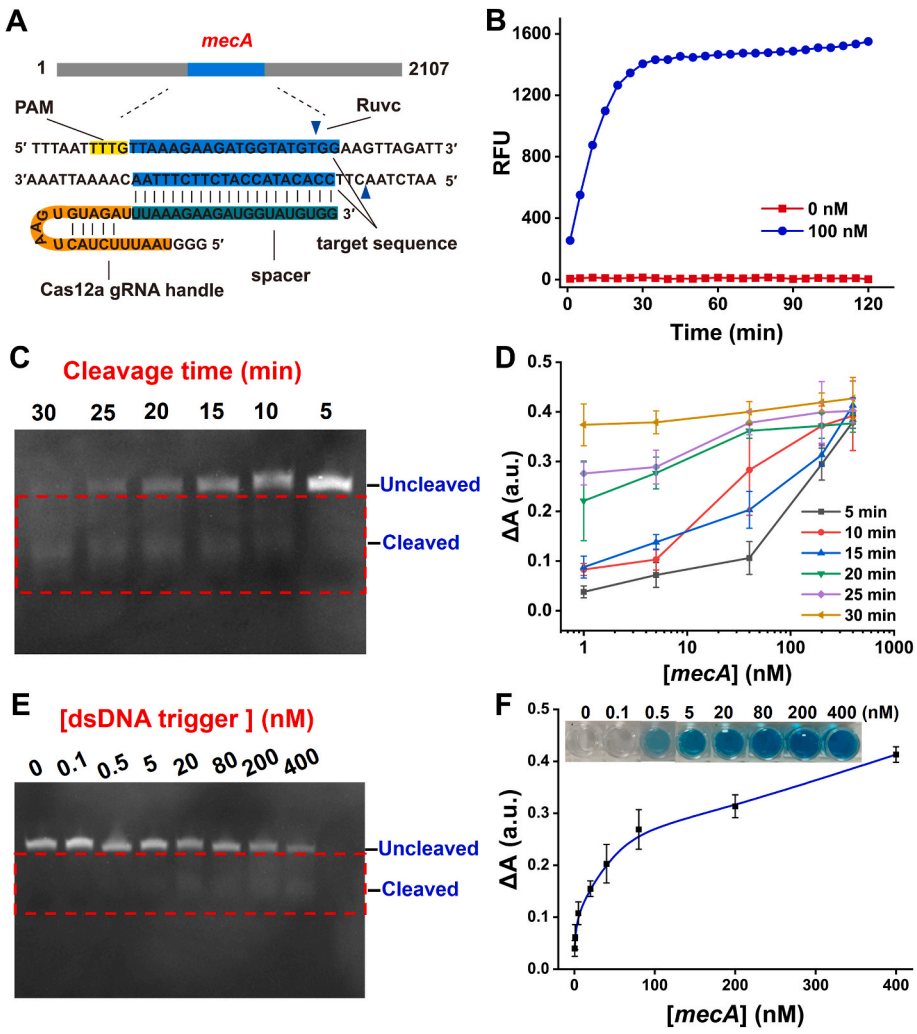

Fig. 2. Feasibility of aptamer-based colorimetry using the CRISPR/Cas12a system. (A) Schematic diagram of site-specific recognition of target sequence. (B) Verification of the effectiveness of designed gRNA using fluorescence method. (C) Polyacrylamide gel electrophoresis of the aptamer with different cleavage time. (D) UV–vis absorption at 652 nm of aptamer-based colorimetric system with different cleavage times. (E) Agarose gel electrophoresis analysis of aptamer with different concentrations of *mecA* dsDNA trigger. (F) UV–vis absorption at 652 nm and corresponding photograph of colorimetric solution initiated by different concentrations of *mecA* dsDNA trigger. Error bars represent the standard deviation of three replicates (n = 3).

of magnitude, respectively; moreover, our method has a more portable and simple signal readout than these instrument-dependent method, thus is suitable for point-of-care testing.

Additionally, analytical specificity was evaluated by analyzing four common bacteria, including MRSA, methicillin-susceptible *Staphylococcus aureus* (MSSA), *Escherichia coli* (*E. coli*), *Listeria monocytogenes* (*L. monocytogenes*), and *Salmonella enteritidis* (*S. enteritidis*). As shown in Fig. 3D, at the same concentration, only MRSA can induce a significant change in characteristic UV–vis absorption, whereas other bacteria exert negligible effects. This outcome proved the high specificity of the method for MRSA detection, which was mainly attributed to the endogenous sequence-specific recognition of the CRISPR/Cas12a system. The excellent sensitivity, specificity, and simplicity, in addition to its visualization, endow the proposed method with superiority in point-of-care testing for bacterial resistance.

3.3. Real samples analysis

The practicability and accuracy of this aptamer-based colorimetric biosensor in the real world were challenged by analyzing 12 suspected MRSA samples isolated from clinical patients. Notably, $\Delta A = 0.1$ was used as the cutoff value to distinguish positive samples from negative samples, which is calculated using the linear equation $Y = 0.064X + 0.094$ $\{X = \log$ [MRSA] (CFU/mL)$\}$ when MRSA is at the detection limit (8 CFU mL^{-1}). $\Delta A > 0.1$ thus represent the MRSA-positive, while $\Delta A < 0.1$ is MRSA-negative. The results show that samples 3, 6, 8, and 12 were tested as MRSA-positive ($\Delta A > 0.1$, blue coloration) using the developed method and the remaining samples were detected as MRSA-negative ($\Delta A < 0.1$, colorless) (Fig. 4A and B). For comparison, these samples were determined by the qPCR method. The samples are quantified by the cycle threshold value (Ct), which represents the number of cycles through which the fluorescence signal in each reaction tube reaches a set value. Not surprisingly, samples 3, 6, 8, and 12 were measured to be positive for MRSA with Ct values of 23, 18, 28, and 26, respectively, while no classical amplification curve was found in other samples (Fig. S7). The consistent results between aptamer-based colorimetry and the standardized qPCR method (Fig. 4C) demonstrated the reliability and accuracy of our method in a real-world application. Significantly, unlike qPCR, our method can be implemented without the cumbersome thermal system and thus is more suitable for off-laboratory testing.

4. Conclusions

In conclusion, an efficient aptamer-based colorimetric biosensor was developed by integrating the powerful CRISPR/Cas12a system and RPA for MRSA detection. With triple amplification, this approach achieved rapid, visual, ultrasensitive, and specific detection of MRSA with a LOD of 8 CFU mL^{-1}. Satisfactory accuracy in analyzing clinical MRSA colonies also indicated its robust applicability. We envision that this biosensor can be easily extended to diagnose disease biomarkers by programming the corresponding gRNA, and it may be amenable to bacterial identification and typing. The fully integrated, sample-to-

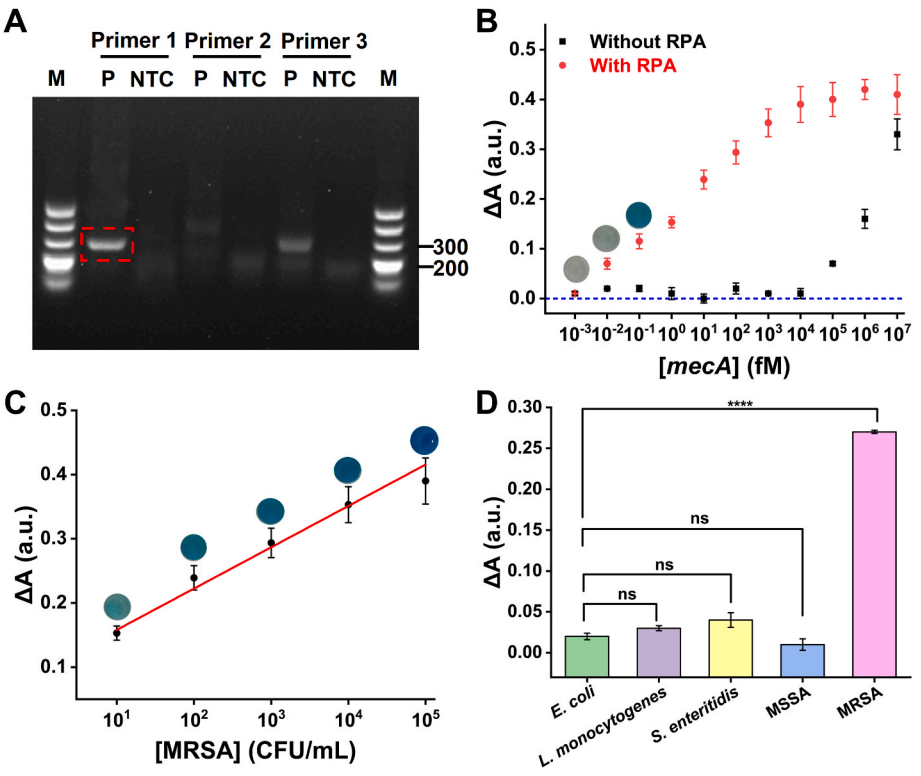

Fig. 3. Sensitivity and specificity of aptamer-based colorimetric detection of MRSA by using CRISPR/Cas12a system and RPA. (A) Screening of RPA primer. P and NTC represent MRSA-positive sample and negative control, respectively. (B) Sensitivity of aptamer-based colorimetric detection of MRSA with and without RPA, inset is the corresponding photograph of detection system. (C) Linear range for MRSA detection using aptamer-based colorimetric biosensor, inset is the corresponding photograph of detection system. (D) Specificity of aptamer-based colorimetric detection of MRSA. Two-tailed Student's t-test; "ns" represents no significance, ****$p < 0.0001$. Error bars represent the standard deviation of three replicates (n = 3).

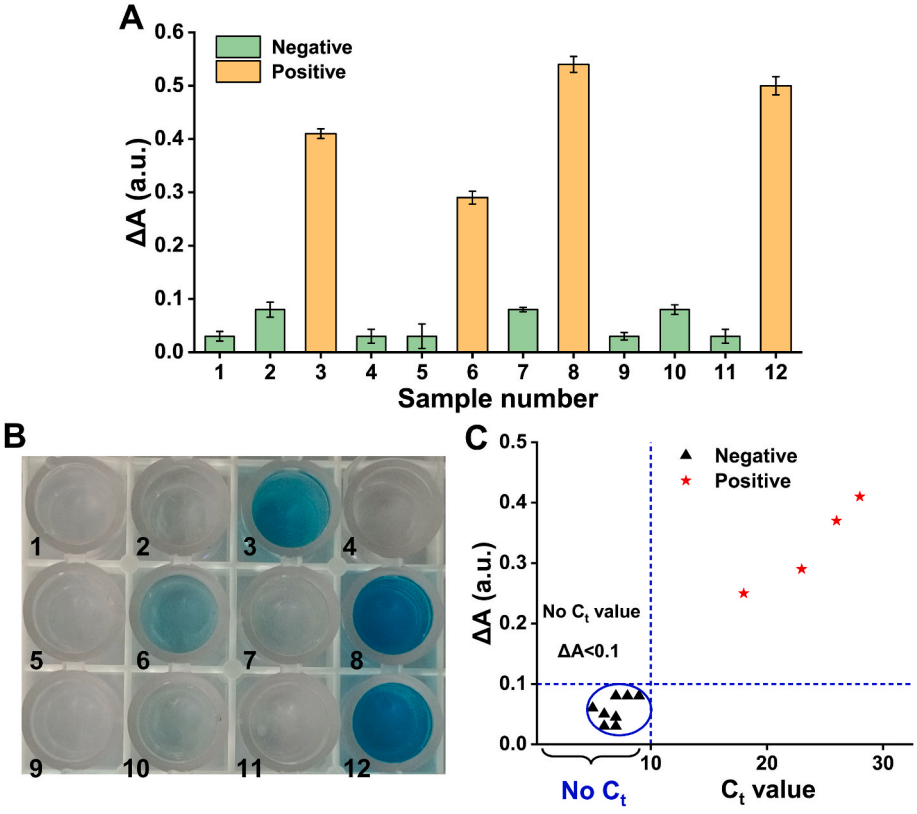

Fig. 4. Capacity of aptamer-based colorimetric biosensor for MRSA detection in real samples. UV–vis absorption at 652 nm (A), and photograph (B) of this aptamer-based colorimetric system. (C) Consistency of the proposed method and qPCR in real samples analysis. $\Delta A = A\text{-}A_0$, A represents the absorbance at 652 nm in the presence of target, A_0 represents the absorbance at 652 nm in the absence of target. Error bars represent the standard deviation of three replicates (n = 3).

result, and multiplexed CRISPR-based strategy is expected to provide further improvement and development.

CRediT authorship contribution statement

Luyu Wei: Methodology, Conceptualization, Investigation, Formal analysis, Writing – original draft, Writing – review & editing. **Zhilong Wang:** Writing – review & editing. **Jia Wang:** Supervision. **Xiaohong Wang:** Supervision, Resources. **Yiping Chen:** Supervision, Conceptualization, Writing – review & editing.

Declaration of competing interest

The authors declare that they have no known competing financial interests or personal relationships that could have appeared to influence the work reported in this paper.

Data availability

Data will be made available on request.

Acknowledgments

The authors thank the Laboratory of Lingnan Modern Agriculture Project (NZ2021036), the National Natural Science Foundation of China (32172293), HZAU-AGIS Cooperation Fund (SZYJY2021002), the Wuhan Science and Technology Planning Project (2020030603012347), and the Key planning project of Hubei Province (2020BBA053) for financial support.

Appendix A. Supplementary data

Supplementary data to this article can be found online at https://doi.org/10.1016/j.aca.2022.340357.

References

[1] A.S. Lee, H. de Lencastre, J. Garau, J. Kluytmans, S. Malhotra-Kumar, A. Peschel, S. Harbarth, Methicillin-resistant *Staphylococcus aureus*, Nat. Rev. Dis. Prim. 4 (2018), 18033, https://doi.org/10.1038/nrdp.2018.34.

[2] Y.H. Lu, Z.L. Yuan, J.R. Bai, Q. Lin, R.J. Deng, A.M. Luo, Y.L. Chi, S. Deng, Q. He, Directly profiling intact *Staphylococcus aureus* in water and foods via enzymatic cleavage aptasensor, Anal. Chim. Acta 1132 (2020) 28–35, https://doi.org/10.1016/j.aca.2020.07.058.

[3] S.R. Harris, E.J. Feil, M.T.G. Holden, M.A. Quail, E.K. Nickerson, N. Chantratita, S. Gardete, A. Tavares, N. Day, J.A. Lindsay, J.D. Edgeworth, H. de Lencastre, et al., Evolution of MRSA during hospital transmission and intercontinental spread, Science 327 (2010) 469–474, https://doi.org/10.1126/science.1182395.

[4] H.F. Chambers, F.R. DeLeo, Waves of resistance: *Staphylococcus aureus* in the antibiotic era, Nat. Rev. Microbiol. 7 (2009) 629–641, https://doi.org/10.1038/nrmicro2200.

[5] O. Baltekin, A. Boucharin, E. Tano, D.I. Andersson, J. Elf, Antibiotic susceptibility testing in less than 30 min using direct single-cell imaging, P. Natl. Acad. Sci. USA 114 (2017) 9170–9175, https://doi.org/10.1073/pnas.1708558114.

[6] N.G. Schoepp, T.S. Schlappi, M.S. Curtis, S.S. Butkovich, S. Miller, R.M. Humphries, R.F. Ismagilov, Rapid pathogen-specific phenotypic antibiotic susceptibility testing using digital LAMP quantification in clinical samples, Sci. Transl. Med. 9 (2017), eaal3693, https://doi.org/10.1126/scitranslmed.aal3693.

[7] H. Li, M. Li, Y. Yang, F. Wang, F. Wang, C. Li, Aptamer-linked CRISPR/Cas12a-based immunoassay, Anal. Chem. 93 (2021) 3209–3216, https://doi.org/10.1021/acs.analchem.0c04687.

[8] M. Goudarzi, S.S. Seyedjavadi, M.J. Nasiri, H. Goudarzi, R. Sajadi Nia, H. Dabiri, Molecular characteristics of methicillin-resistant *Staphylococcus aureus* (MRSA) strains isolated from patients with bacteremia based on MLST, *SCCmec*, *spa*, and *agr* locus types analysis, *Microb.* Pathog. 104 (2017) 328–335, https://doi.org/10.1016/j.micpath.2017.01.055.

[9] M.A. Abdou Mohamed, H.N. Kozlowski, J. Kim, K. Zagorovsky, M. Kantor, J. J. Feld, S. Mubareka, T. Mazzulli, W.C.W. Chan, Diagnosing antibiotic resistance using nucleic acid enzymes and gold nanoparticles, ACS Nano 15 (2021) 9379–9390, https://doi.org/10.1021/acsnano.0c09902.

[10] D.C. Oliveira, H. de Lencastre, Multiplex PCR strategy for rapid identification of structural types and variants of the mec element in methicillin-resistant *Staphylococcus aureus*, Antimicrob. Agents Chemother. 46 (2002) 2155–2161, https://doi.org/10.1128/AAC.46.7.2155-2161.2002.

[11] I. Choopara, A. Suea-Ngam, Y. Teethaisong, P.D. Howes, M. Schmelcher, A. Leelahavanichkul, S. Thunyaharn, D. Wongsawaeng, A.J. DeMello, D. Dean, N. Somboonna, Fluorometric paper-based, loop-mediated isothermal amplification devices for quantitative point-of-care detection of methicillin-resistant *Staphylococcus aureus* (MRSA), ACS Sens. 6 (2021) 742–751, https://doi.org/10.1021/acssensors.0c01405.

[12] B. Deiman, C. Jay, C. Zintilini, S. Vermeer, D. van Strijp, F. Venema, P. van de Wiel, Efficient amplification with NASBA (R) of hepatitis B virus, herpes simplex virus and methicillin resistant *Staphylococcus aureus* DNA, J. Virol. Methods 151 (2008) 283–293, https://doi.org/10.1016/j.jviromet.2008.04.009.

[13] T. Gaj, C.A. Gersbach, C.F. Barbas, ZFN, TALEN, and CRISPR/Cas-based methods for genome engineering, Trends Biotechnol. 31 (2013) 397–405, https://doi.org/10.1016/j.tibtech.2013.04.004.

[14] B. Zetsche, J.S. Gootenberg, O.O. Abudayyeh, I.M. Slaymaker, K.S. Makarova, P. Essletzbichler, S.E. Volz, J. Joung, J. van der Oost, A. Regev, E.V. Koonin, F. Zhang, Cpf1 is a single RNA-guided endonuclease of a class 2 CRISPR-Cas system, Cell 163 (2015) 759–771, https://doi.org/10.1016/j.cell.2015.09.038.

[15] J.S. Chen, E. Ma, L.B. Harrington, M.D. Costa, X. Tian, J.M. Palefsky, J.A. Doudna, CRISPR-Cas12a target binding-unleashes indiscriminate single-stranded DNase activity, Science 360 (2018) 436–439, https://doi.org/10.1126/science.aar6245.

[16] M. Liang, Z. Li, W. Wang, J. Liu, L. Liu, G. Zhu, L. Karthik, M. Wang, K.F. Wang, Z. Wang, J. Yu, Y. Shuai, et al., A CRISPR-Cas12a-derived biosensing platform for the highly sensitive detection of diverse small molecules, Nat. Commun. 10 (2019) 3672, https://doi.org/10.1038/s41467-019-11648-1.

[17] Y. Xiong, J. Zhang, Z. Yang, Q. Mou, Y. Ma, Y. Xiong, Y. Lu, Functional DNA regulated CRISPR-Cas12a sensors for point-of-care diagnostics of non-nucleic-acid targets, J. Am. Chem. Soc. 142 (2020) 207–213, https://doi.org/10.1021/jacs.9b09211.

[18] J.P. Broughton, X. Deng, G. Yu, C.L. Fasching, V. Servellita, J. Singh, X. Miao, J. A. Streithorst, A. Granados, A. Sotomayor-Gonzalez, K. Zorn, A. Gopez, et al., CRISPR-Cas12-based detection of SARS-CoV-2, Nat. Biotechnol. 38 (2020) 870–874, https://doi.org/10.1038/s41587-020-0513-4.

[19] J.S. Gootenberg, O.O. Abudayyeh, M.J. Kellner, J. Joung, J.J. Collins, F. Zhang, Multiplexed and portable nucleic acid detection platform with Cas13, Cas12a, and Csm6, Science 360 (2018) 439, https://doi.org/10.1126/science.aaq0179. -+.

[20] Y. Dai, R.A. Somoza, L. Wang, J.F. Welter, Y. Li, A.I. Caplan, C.C. Liu, Exploring the *trans*-cleavage activity of CRISPR-Cas12a (cpf1) for the development of a universal electrochemical biosensor, Angew. Chem., Int. Ed. 58 (2019) 17399–17405, https://doi.org/10.1002/anie.201910772.

[21] J. Liu, J. Chen, D. Wu, M. Huang, J. Chen, R. Pan, Y. Wu, G. Li, CRISPR-/Cas12a-mediated liposome-amplified strategy for the surface-enhanced Raman scattering and naked-eye detection of nucleic acid and application to food authenticity screening, Anal. Chem. 93 (2021) 10167–10174, https://doi.org/10.1021/acs.analchem.1c01163.

[22] J.S. Park, K. Hsieh, L. Chen, A. Kaushik, A.Y. Trick, T.H. Wang, Digital CRISPR/Cas-assisted assay for rapid and sensitive detection of SARS-CoV-2, Adv. Sci. 8 (2021), 2003564, https://doi.org/10.1002/advs.202003564.

[23] H. Yue, B. Shu, T. Tian, E. Xiong, M. Huang, D. Zhu, J. Sun, Q. Liu, S. Wang, Y. Li, X. Zhou, Droplet Cas12a assay enables DNA quantification from unamplified samples at the single-molecule level, Nano Lett. 21 (2021) 4643–4653, https://doi.org/10.1021/acs.nanolett.1c00715.

[24] J.H. Choi, J. Lim, M. Shin, S.H. Paek, J.W. Choi, CRISPR-Cas12a-based nucleic acid amplification-free DNA biosensor via Au nanoparticle-assisted metal-enhanced fluorescence and colorimetric analysis, Nano Lett. 21 (2021) 693–699, https://doi.org/10.1021/acs.nanolett.0c04303.

[25] Y. Jiang, M. Hu, A.A. Liu, Y. Lin, L. Liu, B. Yu, X. Zhou, D.W. Pang, Detection of SARS-CoV-2 by CRISPR/Cas12a-enhanced colorimetry, ACS Sens. 6 (2021) 1086–1093, https://doi.org/10.1021/acssensors.0c02365.

[26] C. Yuan, T. Tian, J. Sun, M. Hu, X. Wang, E. Xiong, M. Cheng, Y. Bao, W. Lin, J. Jiang, C. Yang, Q. Chen, et al., Universal and naked-eye gene detection platform based on the clustered regularly interspaced short palindromic repeats/Cas12a/13a system, Anal. Chem. 92 (2020) 4029–4037.

[27] R. Liu, Y. Hu, Y. He, T. Lan, J. Zhang, Translating daily COVID-19 screening into a simple glucose test: a proof of concept study, Chem. Sci. 12 (2021) 9022–9030, https://doi.org/10.1039/D1SC00512J.

[28] R. Nouri, Y. Jiang, Z. Tang, X.L. Lian, W. Guan, Detection of SARS-CoV-2 with solid-state CRISPR-Cas12a-assisted nanopores, Nano Lett. 21 (2021) 8393–8400, https://doi.org/10.1021/acs.nanolett.1c02974.

[29] Y.H. Lin, W.L. Tseng, Highly sensitive and selective detection of silver ions and silver nanoparticles in aqueous solution using an oligonucleotide-based fluorogenic probe, Chem. Commun. (2009) 6619–6621, https://doi.org/10.1039/B915990H.

[30] A. Ono, S. Cao, H. Togashi, M. Tashiro, T. Fujimoto, T. Machinami, S. Oda, Y. Miyake, I. Okamoto, Y. Tanaka, Specific interactions between silver(I) ions and cytosine-cytosine pairs in DNA duplexes, Chem. Commun. (2008) 4825–4827, https://doi.org/10.1039/b808686a.

[31] H.L. Tian, Y. Meng, S. Zhao, W.Y. Mi, H. Ji, Z.P. Wang, Detection of Ag^{+} based on aggregation-induced emission fluorescent aptasensor, Food Sci. (N. Y.) 40 (2019) 347–351, https://doi.org/10.7506/spkx1002-6630-20180823-243.

[32] M. Luo, X. Xue, H. Rao, H. Wang, X. Liu, X. Zhou, Z. Xue, X. Lu, Simply converting color signal readout into thermal signal readout for breaking the color resolution limitation of colorimetric sensor, Sens. Actuators, B 309 (2020), 127707, https://doi.org/10.1016/j.snb.2020.127707.

[33] H. Arakawa, R. Ahmad, M. Naoui, H.A. Tajmir-Riahi, A comparative study of calf thymus DNA binding to Cr(III) and Cr(VI) ions-Evidence for the guanine N-7-chromium-phosphate chelate formation, J. Biol. Chem. 275 (2000) 10150–10153, https://doi.org/10.1074/jbc.275.14.10150.

[34] H. Torigoe, Y. Miyakawa, A. Ono, T. Kozasa, Thermodynamic properties of the specific binding between Ag^+ ions and C:C mismatched base pairs in duplex DNA, Nucleos Nucleot. Nucleic Acids 30 (2011) 149–167, https://doi.org/10.1080/15257770.2011.553210.

[35] S. Monecke, E. Mueller, S.D. Braun, M. Armengol-Porta, M. Bes, S. Boswihi, M. El-Ashker, I. Engelmann, D. Gawlik, M. Gwida, H. Hotzel, R. Nassar, et al., Characterisation of *S. aureus*/MRSA CC1153 and review of mobile genetic elements carrying the fusidic acid resistance gene fusC, Sci. Rep. 11 (2021) 8128, https://doi.org/10.1038/s41598-021-86273-4.

[36] K. Vanamala, K. Tatiparti, K. Bhise, S. Sau, M.H. Scheetz, M.J. Rybak, D. Andes, A. K. Iyer, Novel approaches for the treatment of methicillin-resistant *Staphylococcus aureus*: using nanoparticles to overcome multidrug resistance, Drug Discov. Today 26 (2020) 31–43, https://doi.org/10.1016/j.drudis.2020.10.011.